

# Higgs $p_T$ Spectrum and Total Cross Section with Fiducial Cuts at Third Resummed and Fixed Order in QCD

Georgios Billis,<sup>1</sup> Bahman Dehnadi,<sup>1</sup> Markus A. Ebert,<sup>2</sup> Johannes K. L. Michel,<sup>3</sup> and Frank J. Tackmann<sup>1</sup>

<sup>1</sup>*Deutsches Elektronen-Synchrotron (DESY), D-22607 Hamburg, Germany*

<sup>2</sup>*Max-Planck-Institut für Physik, Föhringer Ring 6, 80805 München, Germany*

<sup>3</sup>*Center for Theoretical Physics, Massachusetts Institute of Technology, Cambridge, Massachusetts 02139, USA*

(Dated: February 15, 2021)

We present predictions for the gluon-fusion Higgs  $p_T$  spectrum at third resummed and fixed order ( $N^3LL'+N^3LO$ ) including fiducial cuts as required by experimental measurements at the Large Hadron Collider. Integrating the spectrum, we predict for the first time the total fiducial cross section to third order ( $N^3LO$ ) and improved by resummation. The  $N^3LO$  correction is enhanced by cut-induced logarithmic effects and is not reproduced by the inclusive  $N^3LO$  correction times a lower-order acceptance. These are the highest-order predictions of their kind achieved so far at a hadron collider.

## I. INTRODUCTION

Fiducial and differential cross-section measurements of the discovered Higgs boson [1, 2] provide the most model-independent way to study Higgs production at the Large Hadron Collider. They are thus central to its physics program [3–15] and will remain so in the future [16].

Theoretical predictions for the dominant gluon-fusion ( $gg \rightarrow H$ ) Higgs production mode suffer from large perturbative corrections. This has led to the calculation of the total inclusive production cross section to third order ( $N^3LO$ ) [17–25], which is made possible by treating the decay of the Higgs boson fully inclusively. Unfortunately, this also makes it a primarily theoretical quantity; one that cannot be measured in experiment. The experimental measurements necessarily involve kinematic selection and acceptance cuts on the Higgs decay products, which reduce the cross section by an  $\mathcal{O}(1)$  amount. Therefore, any comparison of theory and experiment always involves a prediction of the *fiducial* cross section, i.e., the cross section within the experimental acceptance. Currently, the fiducial cross section for  $gg \rightarrow H$  is only known to second order (NNLO). A key challenge is to calculate it at  $N^3LO$ , which we do here for the first time. To be specific, we consider  $H \rightarrow \gamma\gamma$  with the fiducial cuts used by ATLAS [8, 26],

$$\begin{aligned} p_T^{\gamma 1} &\geq 0.35 m_H, & p_T^{\gamma 2} &\geq 0.25 m_H, \\ |\eta^\gamma| &\leq 1.37 \quad \text{or} \quad 1.52 \leq |\eta^\gamma| \leq 2.37. \end{aligned} \quad (1)$$

Arguably, the most important differential cross section of the Higgs boson is its transverse-momentum ( $q_T$ ) distribution, serving as a benchmark spectrum in many experimental analyses. At finite  $q_T$ , it is known to NNLO<sub>1</sub> [27–36], i.e., from calculating  $H + 1$  parton to NNLO, including fiducial cuts, which is an important ingredient for our results. For  $q_T \ll m_H$ , the  $q_T$  spectrum contains large Sudakov logarithms of  $q_T/m_H$ , which must be resummed to all orders in perturbation theory to obtain precise and reliable predictions. So far, this re-

summation has been achieved to NNLL' and  $N^3LL$  [37–44], which include second and third order evolution and which capture in particular all  $\mathcal{O}(\alpha_s^2)$  contributions that are singular for  $q_T \rightarrow 0$ . This is also the basis of the  $q_T$  subtraction method for NNLO calculations [45].

In this Letter, we obtain for the first time the resummed  $q_T$  spectrum at  $N^3LL'+N^3LO$ , both inclusively and with fiducial cuts. This is the highest order achieved to date for a differential distribution at a hadron collider. Compared to  $N^3LL$ , the resummation at  $N^3LL'$  incorporates the complete  $\mathcal{O}(\alpha_s^3)$  singular structure for  $q_T \rightarrow 0$ , i.e., all 3-loop virtual and corresponding real corrections, allowing us to consistently match to  $N^3LO$ . We incorporate the fiducial cuts in the resummed  $q_T$  spectrum following the recent analysis in Ref. [46]. This allows us to also resum large, so-called fiducial power corrections induced by the fiducial cuts [46, 47], and eventually to predict the total fiducial cross section at  $N^3LO$  from the integral of the resummed fiducial  $q_T$  spectrum. This constitutes the first complete application of  $q_T$  subtractions at this order. (For earlier results and discussions see Refs. [48, 49].)

The total inclusive cross section can be considered independently of the  $q_T$  spectrum. In particular, the  $q_T$  resummation effects in the inclusive spectrum formally cancel in its integral. This cancellation is broken by the fiducial power corrections, causing leftover logarithmic contributions in the total fiducial cross section which worsen its perturbative behavior. They are resummed by integrating the resummed spectrum, restoring the perturbative convergence. Hence, the fiducial  $q_T$  spectrum is now the more fundamental quantity, while the total fiducial cross section becomes a derived quantity.

## II. $q_T$ RESUMMATION WITH FIDUCIAL POWER CORRECTIONS

We work in the narrow-width limit and factorize the cross section into Higgs production and decay,

$$\frac{d\sigma}{dq_T} = \int dY A(q_T, Y; \Theta) W(q_T, Y). \quad (2)$$

Since the Higgs is a scalar boson, Eq. (2) contains a single hadronic structure function  $W(q_T, Y)$  encoding the  $gg \rightarrow H$  production process. As  $W$  is a Lorentz-scalar function and inclusive over the hadronic final state, it can only depend on the Higgs momentum  $q^\mu$  and the proton momenta  $P_{a,b}^\mu$  via  $q^2 = m_H^2$  and  $2q \cdot P_{a,b} = E_{\text{cm}} \sqrt{m_H^2 + \vec{q}_T^2} e^{\mp Y}$ , where  $Y$  and  $\vec{q}_T$  are the Higgs rapidity and transverse momentum. Its only nontrivial dependence is thus on  $Y$  and  $q_T = |\vec{q}_T|$ . The function  $A(q_T, Y; \Theta)$  in Eq. (2) encodes the Higgs decay including fiducial cuts, collectively denoted by  $\Theta$ . It corresponds to the fiducial acceptance point by point in  $q_T$  and  $Y$ , such that in the inclusive case without cuts  $A_{\text{incl}}(q_T, Y) = 1$ . Hence,  $W$  is equivalent to the inclusive spectrum.

Let us expand the  $q_T$  spectrum in powers of  $q_T/m_H$ ,

$$\begin{aligned} \frac{d\sigma}{dq_T} &= \frac{d\sigma^{(0)}}{dq_T} + \frac{d\sigma^{(1)}}{dq_T} + \frac{d\sigma^{(2)}}{dq_T} + \dots \\ &\sim \frac{1}{q_T} \left[ \mathcal{O}(1) + \mathcal{O}\left(\frac{q_T}{m_H}\right) + \mathcal{O}\left(\frac{q_T^2}{m_H^2}\right) + \dots \right]. \end{aligned} \quad (3)$$

The singular, leading-power term  $d\sigma^{(0)}/dq_T$  scales as  $1/q_T$  and dominates for  $q_T \ll m_H$ . It contains  $\delta(q_T)$  and  $[\ln^n(q_T/m_H)/q_T]_+$  distributions encoding the cancellation of real and virtual infrared singularities at  $q_T = 0$ . The  $d\sigma^{(n \geq 1)}/dq_T$  are called power corrections.

Because of azimuthal symmetry,  $W(q_T, Y)$  only receives quadratic power corrections [46, 50],

$$W(q_T, Y) = W^{(0)}(q_T, Y) + W^{(2)}(q_T, Y) + \dots, \quad (4)$$

where  $W^{(0)} \sim 1/q_T$  contains the singular terms. The acceptance corrections are finite at  $q_T = 0$ , but the fiducial cuts generically break azimuthal symmetry such that it receives linear power corrections [46, 47],

$$A(q_T, Y; \Theta) = A(0, Y; \Theta) \left[ 1 + \mathcal{O}\left(\frac{q_T}{m_H}\right) \right]. \quad (5)$$

The strict leading-power spectrum is thus given by

$$\frac{d\sigma^{(0)}}{dq_T} = \int dY A(0, Y; \Theta) W^{(0)}(q_T, Y). \quad (6)$$

The fiducial power corrections,

$$\frac{d\sigma^{\text{fpc}}}{dq_T} = \int dY \left[ A(q_T, Y; \Theta) - A(0, Y; \Theta) \right] W^{(0)}(q_T, Y), \quad (7)$$

were analyzed in Refs. [46, 47]. They include all linear power corrections  $d\sigma^{(1)}/dq_T$  and are absent in the

inclusive spectrum. They are quite subtle, and can be further enhanced to  $\mathcal{O}(q_T/p_L)$ , where  $p_L$  is an effective kinematic scale set by the fiducial cuts with typically  $p_L \ll m_H$ . This prohibits expanding  $A(q_T, Y; \Theta)$  even for  $q_T \ll m_H$  once  $q_T \sim p_L$ . For example, for the photon  $p_T^{\text{cut}}, p_L \sim m_H - 2p_T^{\text{cut}}$ . For the cuts in Eq. (1), the expansion of  $A$  starts failing for  $q_T \gtrsim 10$  GeV, where the inclusive power corrections from  $W^{(2)}$  are at the few-percent level. It is thus critical to use the exact  $q_T$ -dependent acceptance and take

$$\frac{d\sigma^{\text{sing}}}{dq_T} = \int dY A(q_T, Y; \Theta) W^{(0)}(q_T, Y) \quad (8)$$

as the leading ‘‘singular’’ contribution at small  $q_T$ , corresponding to the sum of Eqs. (6) and (7). The remaining ‘‘nonsingular’’ contributions,

$$\frac{d\sigma^{\text{nons}}}{dq_T} = \int dY A(q_T, Y; \Theta) \left[ W^{(2)}(q_T, Y) + \dots \right], \quad (9)$$

are then suppressed by  $\mathcal{O}(q_T^2/m_H^2)$ .

In general, and for the ATLAS cuts in particular,  $A(q_T, Y; \Theta)$  is a very nasty function given by a boosted phase-space integral over a conjunction of complicated  $\theta$  functions encoding all cuts. Nevertheless, using a dedicated semianalytic algorithm we are able to evaluate it with sufficient numerical speed and accuracy.

As  $A$  itself does not contain large logarithms, resumming  $W^{(0)}$  in Eq. (8) correctly resums also the fiducial power corrections in Eq. (7) to the same order [46]. The resummation of  $W^{(0)}$  is equivalent to that of the leading-power inclusive spectrum, and follows from its factorization theorem originally derived in Refs. [51–53] or equivalent formulations [54–60]. We employ soft-collinear effective theory [61–65] with rapidity renormalization [58, 66] using the exponential regulator [60], where

$$\begin{aligned} W^{(0)}(q_T, Y) &= H(m_H^2, \mu) \int d^2\vec{k}_a d^2\vec{k}_b d^2\vec{k}_s \delta(q_T - |\vec{k}_a + \vec{k}_b + \vec{k}_s|) \\ &\quad \times B_g^{\mu\nu}(x_a, \vec{k}_a, \mu, \nu) B_{g\mu\nu}(x_b, \vec{k}_b, \mu, \nu) S(\vec{k}_s, \mu, \nu). \end{aligned} \quad (10)$$

The hard function  $H$  contains the effective  $gg \rightarrow H$  form factor. The beam functions  $B_g^{\mu\nu}$  describe collinear radiation with total transverse momentum  $\vec{k}_{a,b}$  and longitudinal momentum fractions  $x_{a,b} = (m_H/E_{\text{cm}})e^{\pm Y}$ . The soft function  $S$  describes soft radiation with total transverse momentum  $\vec{k}_s$ .

All functions in Eq. (10) are renormalized objects, with  $\mu$  and  $\nu$  denoting their virtuality and rapidity renormalization scales. The all-order resummation follows by first evaluating each function at fixed order at its own natural boundary scale(s)  $\mu_{H,B,S}, \nu_{B,S}$ . These boundary conditions are then evolved to a common (arbitrary) point in  $\mu$  and  $\nu$  by solving the coupled system of renormalization

group equations. The exact solution for the  $q_T$  distribution is formally equivalent [67] to the canonical solution in conjugate ( $b_T$ ) space, which is the approach we follow here; see Refs. [46, 67, 68] for details. At  $N^3LL'$  ( $N^3LL$ ) we require the  $N^3LO$  (NNLO) boundary conditions for the hard [69–73] and beam and soft functions [49, 74–78], the 3-loop noncusp anomalous dimensions [49, 74, 75, 79–82], and the 4-loop  $\beta$  function [83–86] and gluon cusp anomalous dimension [87–93]. At NNLL, all ingredients enter at one order lower than at  $N^3LL$ .

The 3-loop beam function boundary terms have been computed only recently [77, 78]. They involve a plethora of harmonic polylogarithms up to weight five with non-trivial rational prefactors, which must be convolved against the PDFs. This makes a naive implementation too slow and numerically unstable. Instead, we obtain fast numerical implementations for all kernels at close to double precision using a dedicated algorithm that separates an entire kernel into pieces with only single branch cuts, which then admit suitable, fast-converging logarithmic expansions around  $z = 0$  and  $z = 1$ .

The hard function  $H$  contains timelike logarithms  $\ln[(-m_H^2 - i0)/\mu^2]$ , which are resummed by using an imaginary boundary scale  $\mu_H = -im_H$ . This significantly improves the perturbative convergence compared to the spacelike choice  $\mu_H = m_H$  [94–98]. It is advantageous to apply this timelike resummation not just to  $W^{(0)}$ , which contains  $H$  naturally, but also to the full  $W(q_T, Y)$ , as demonstrated for the rapidity spectrum in Ref. [73], or equivalently the nonsingular corrections, as in similar contexts [81, 99]. To do so, we take [73]

$$W(q_T, Y) = H(m_H^2, \mu_{FO}) \left[ \frac{W(q_T, Y)}{H(m_H^2, \mu_{FO})} \right]_{FO}, \quad (11)$$

and analogously for  $d\sigma^{\text{nons}}/dq_T$ . The ratio in square brackets is expanded to fixed order in  $\alpha_s(\mu_{FO})$ , while  $H(m_H^2, \mu_{FO})$  in front is evolved from  $\mu_H$  to  $\mu_{FO}$  at the same order as in Eq. (10). This yields substantial improvements up to  $q_T \sim 200$  GeV, which is not unexpected, as  $W^{(2)}$  will contain  $H$  in parts of its factorization. (Beyond  $q_T \gtrsim 200$  GeV, a dynamic hard scale  $\sim q_T$  becomes more appropriate and the heavy-top limit breaks down, indicating that the hard interaction has become completely unrelated to the  $H + 0$ -parton process.)

The fixed-order coefficients of  $d\sigma^{\text{nons}}/dq_T$  for  $q_T > 0$  are obtained as

$$\frac{d\sigma_{FO}^{\text{nons}}}{dq_T} = \frac{d\sigma_{FO_1}}{dq_T} - \frac{d\sigma_{FO}^{\text{sing}}}{dq_T}. \quad (12)$$

At  $N^nLO$  ( $\equiv N^nLO_0$ ), or  $\mathcal{O}(\alpha_s^n)$  relative to the LO Born cross section, we need the full spectrum at  $N^{n-1}LO_1$ . At  $LO_1$  and  $NLO_1$ , we integrate our own analytic implementation of  $W(q_T, Y)$  against  $A(q_T, Y; \Theta)$ , allowing us to reach  $10^{-4}$  relative precision down to  $q_T = 0.1$  GeV

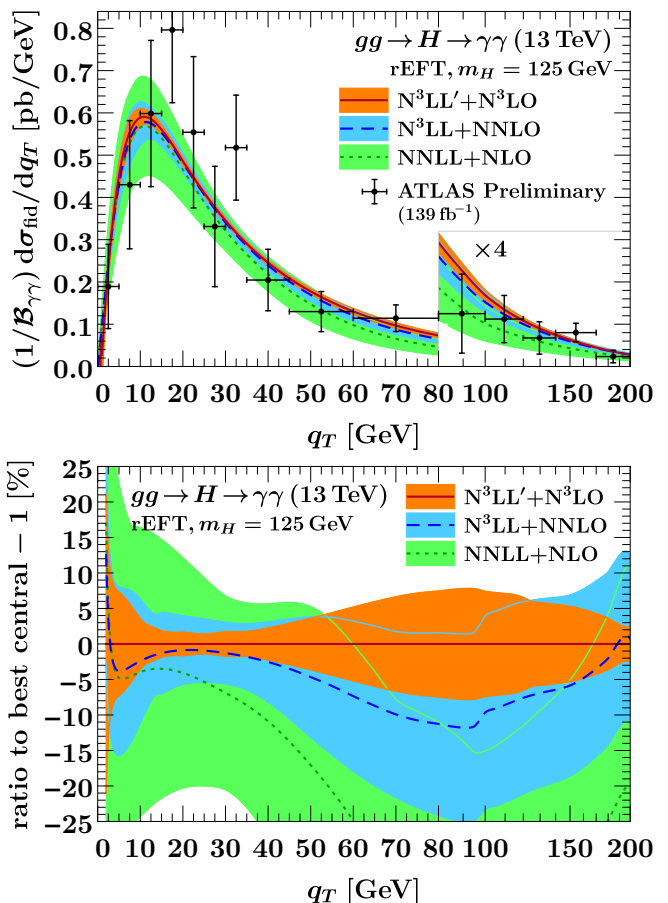


FIG. 1. The  $gg \rightarrow H$   $q_T$  spectrum up to  $N^3LL'+N^3LO$  compared to preliminary ATLAS measurements [26].

at little computational cost. At  $NLO_1$ , we implement results from Ref. [100] after performing the necessary renormalization. The implementation is checked against the numerical code from Ref. [29]. At  $NNLO_1$ , we use existing results [41, 42] from  $NNLOjet$  [30, 34] (see below).

The final resummed  $q_T$  spectrum is then given by

$$\frac{d\sigma}{dq_T} = \frac{d\sigma^{\text{sing}}}{dq_T} + \frac{d\sigma^{\text{nons}}}{dq_T}. \quad (13)$$

While for  $q_T \ll m_H$ , the singular and nonsingular contributions can be considered separately, this separation becomes meaningless for  $q_T \sim m_H$ . To obtain a valid prediction there, the  $q_T$  resummation is switched off, only keeping the timelike resummation, by choosing common boundary scales  $\mu_{S,B} = \nu_{S,B} = i\mu_H = \mu_{FO}$ , such that singular and nonsingular exactly recombine at fixed order into the full result. We use  $q_T$ -dependent profile scales [46, 99, 101] to enforce the correct  $q_T$  resummation for  $q_T \ll m_H$  and smoothly turn it off toward  $q_T \sim m_H$ .

We identify several sources of perturbative uncertainties, namely fixed-order ( $\Delta_{FO}$ ),  $q_T$  resummation ( $\Delta_{q_T}$ ), timelike resummation ( $\Delta_\varphi$ ), and matching uncertainties ( $\Delta_{\text{match}}$ ), which are estimated via appropriate scale variations as detailed in Refs. [46, 73]. They are consid-

ered independent sources and are consequently added in quadrature to obtain the total uncertainty. We neglect nonperturbative effects at small  $q_T$ , which are expected to be  $\sim \Lambda_{\text{QCD}}^2/q_T^2$  and smaller than the current perturbative uncertainties.

Our numerical results are obtained with SCETlib [102]. We use the PDF4LHC15 NNLO parton distribution functions (PDFs) [103],  $\alpha_s(m_Z) = 0.118$ ,  $\mu_{\text{FO}} = m_H = 125$  GeV. We work in the heavy-top limit rescaled with the exact LO dependence on  $m_t = 172.5$  GeV (rEFT). By default, we exclude the  $H \rightarrow \gamma\gamma$  branching ratio ( $\mathcal{B}_{\gamma\gamma}$ ) from our predictions,  $\sigma \equiv \sigma_{\text{fid}}/\mathcal{B}_{\gamma\gamma}$ . Our  $q_T$  spectrum at N<sup>3</sup>LL'+N<sup>3</sup>LO is presented in Fig. 1, showing excellent perturbative convergence. Below  $q_T \lesssim 10$  GeV, this would not be the case without resumming the fiducial power corrections. We also compare to preliminary ATLAS measurements [26], for which we subtract the non-gluon-fusion background and divide by the photon isolation efficiency [8] and  $\mathcal{B}_{\gamma\gamma}$ .

### III. TOTAL FIDUCIAL CROSS SECTION

If (and only if) the singular distributional structure of  $d\sigma^{(0)}/dq_T$  is known, the  $q_T$  spectrum can be integrated to obtain the total cross section. This is the basis of  $q_T$  subtractions [45],

$$\sigma = \sigma^{\text{sub}}(q_T^{\text{off}}) + \int dq_T \left[ \frac{d\sigma}{dq_T} - \frac{d\sigma^{\text{sub}}}{dq_T} \theta(q_T \leq q_T^{\text{off}}) \right]. \quad (14)$$

Here,  $d\sigma^{\text{sub}} = d\sigma^{(0)}[1 + \mathcal{O}(q_T/m_H)]$  contains the singular terms, with  $\sigma^{\text{sub}}(q_T^{\text{off}})$  its distributional integral over  $q_T \leq q_T^{\text{off}}$ , while the term in brackets is numerically integrable. Taking  $\sigma^{\text{sub}} \equiv \sigma^{\text{sing}}$ , we get

$$\sigma = \sigma^{\text{sing}}(q_T^{\text{off}}) + \int_0^{q_T^{\text{off}}} dq_T \frac{d\sigma^{\text{nons}}}{dq_T} + \int_{q_T^{\text{off}}} dq_T \frac{d\sigma}{dq_T}, \quad (15)$$

which is exactly the integral of Eq. (13). The subtractions here are differential in  $q_T$ , where  $q_T^{\text{off}} \sim 10\text{--}100$  GeV determines the range over which they act and exactly cancels between all terms.

To integrate  $d\sigma^{\text{nons}}/dq_T$  in Eq. (15) down to  $q_T = 0$ , we parametrize the fixed-order coefficients in Eq. (12) by their leading behavior,

$$q_T \frac{d\sigma_{\text{FO}}^{\text{nons}}}{dq_T} \Big|_{\alpha_s^n} = \frac{q_T^2}{m_H^2} \sum_{k=0}^{2n-1} \left( a_k + b_k \frac{q_T}{m_H} + \dots \right) \ln^k \frac{q_T^2}{m_H^2}, \quad (16)$$

and perform a fit to this parametrization, which we then integrate analytically. We follow the fit procedure discussed in detail in Refs. [104, 105] including the selection of fit parameters and range, extended to the present case. In particular, to obtain reliable, unbiased fit results, we must account for the uncertainties in the parametrization from yet higher-power corrections. This is done

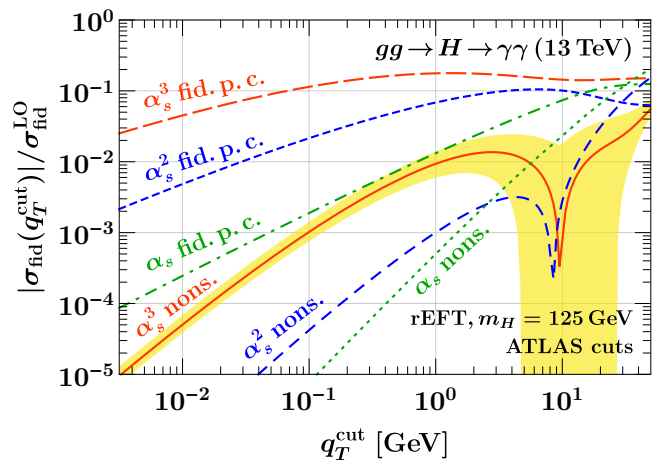


FIG. 2. Fiducial and nonsingular power corrections integrated up to  $q_T \leq q_T^{\text{cut}}$ . The yellow band shows  $\Delta_{\text{nons}}$  from the fit.

by including the next higher-power coefficients ( $b_k, \dots$ ) as nuisance parameters to the extent required by the fit range and precision. In the fiducial case, all  $b_k$  coefficients are required. The fit has been validated extensively. As a benchmark, we correctly reproduce the  $\alpha_s$  ( $\alpha_s^2$ ) coefficients of the total inclusive cross section to better than  $10^{-5}$  ( $10^{-4}$ ) relative precision.

At N<sup>3</sup>LO, we use existing NNLOjet results [41, 42] to get nonsingular data for  $0.74$  GeV ( $4$  GeV)  $\leq q_T \leq q_T^{\text{off}}$  for inclusive log bins (for inclusive and fiducial linear bins). While these data are not yet precise enough toward small  $q_T$  to give a stable fit on their own, we exploit that in the inclusive case, the known  $\alpha_s^3$  coefficient of the total inclusive cross section [25, 106] provides a sufficiently strong additional constraint to obtain a reliable fit. In the fiducial case, we exploit that the inclusive and fiducial  $a_k$  are related, arising from the same  $Y$ -dependent coefficient functions integrated either inclusively or against  $A(0, Y; \Theta)$ . At NLO and NNLO, their ratios lie between 0.4 and 0.55. At N<sup>3</sup>LO, we thus perform a simultaneous fit to inclusive and fiducial data, using 12 fiducial and 8 inclusive parameters, with a loose  $1\sigma$  constraint on the fiducial  $a_k$  to be 0.4–0.55 times their inclusive counterparts. (The  $b_k, \dots$  parameters are unrelated and unconstrained.) We stress that this does not amount to rescaling any part of the fiducial NNLO cross section with an inclusive N<sup>3</sup>LO  $K$  factor. It merely tells the fit to only consider  $a_k$  of roughly the right expected size. This is sufficient to break degeneracies and yields a stable fit, with an acceptable  $\sim 0.1$  pb uncertainty for the fiducial nonsingular integral ( $\Delta_{\text{nons}}$ ).

The often-used  $q_T$  slicing approach amounts to taking  $q_T^{\text{off}} \rightarrow q_T^{\text{cut}} \sim 1$  GeV and simply dropping the power corrections below  $q_T^{\text{cut}}$ . The nonsingular and fiducial power corrections are shown in Fig. 2. The latter are huge at  $\alpha_s^3$ , and even at  $\alpha_s^2$  only become really negligible below  $q_T^{\text{cut}} \lesssim 10^{-2}$  GeV. This is why it is critical for us to

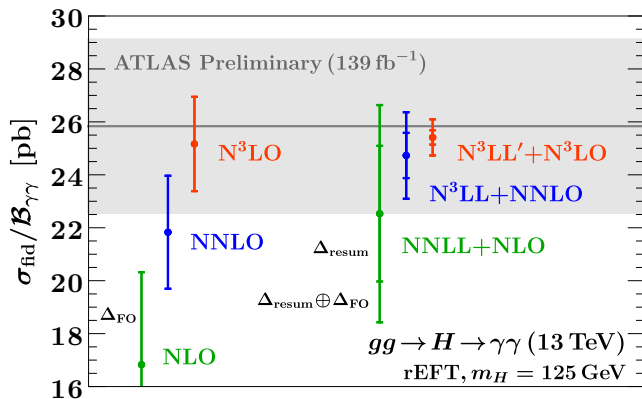


FIG. 3. Total fiducial  $gg \rightarrow H \rightarrow \gamma\gamma$  cross section at fixed  $N^3\text{LO}$  (this work) and including resummation (also this work), where  $\Delta_{\text{resum}} \equiv \Delta_{q_T} \oplus \Delta_{\varphi} \oplus \Delta_{\text{match}}$ , compared to preliminary ATLAS measurements [26].

include them in the subtractions (and to resum them). The remaining nonsingular corrections at  $\alpha_s^3$  are about 10 times larger than at  $\alpha_s^2$ , and at  $q_T^{\text{cut}} = 1\text{--}5\text{ GeV}$  still contribute 5%–10% of the total  $\alpha_s^3$  coefficient. Together with the current precision of the nonsingular data, this makes the above differential subtraction procedure essential to our results.

Evaluating Eq. (15) either at fixed order or including resummation, we obtain our final results for the total fiducial cross section presented in Fig. 3. The poor convergence at fixed order is largely due to the fiducial power corrections. To see this,

$$\begin{aligned} \sigma_{\text{incl}}^{\text{FO}} &= 13.80 [1 + 1.291 + 0.783 + 0.299] \text{ pb}, \\ \sigma_{\text{fid}}^{\text{FO}}/\mathcal{B}_{\gamma\gamma} &= 6.928 [1 + (1.300 + 0.129_{\text{fpc}}) \\ &\quad + (0.784 - 0.061_{\text{fpc}}) \\ &\quad + (0.331 + 0.150_{\text{fpc}})] \text{ pb}. \end{aligned} \quad (17)$$

The successive terms are the contributions from each order in  $\alpha_s$ . The numbers with “fpc” subscript are the contributions of the fiducial power corrections in Eq. (7) integrated over  $q_T \leq 130\text{ GeV}$ . The corrections without them are almost identical to the inclusive case. The fiducial power corrections break this would-be universal acceptance effect, causing a 10% correction at NLO and NNLO and a 50% correction at  $N^3\text{LO}$  and showing no perturbative convergence.

Integrating  $W^{(0)}$  over  $q_T$ , all  $q_T$  logarithms and resummation effects formally have to cancel. (Numerically, this strongly depends on the specific implementation of resummation and matching. We have verified explicitly that it is well satisfied in our approach.) For the fiducial power corrections, the nontrivial  $q_T$  dependence of the acceptance spoils this cancellation and induces residual logarithmic dependence on  $p_L/m_H$  in the integral. This causes the large corrections in Eq. (17), which get resummed using the resummed  $\sigma^{\text{sing}}$  in Eq. (15). Together

with timelike resummation, this leads to the excellent convergence of the resummed results in Fig. 3, very similar to the inclusive case [73],

$$\begin{aligned} \sigma_{\text{incl}} &= 24.16 [1 + 0.756 + 0.207 + 0.024] \text{ pb}, \\ \sigma_{\text{fid}}/\mathcal{B}_{\gamma\gamma} &= 12.89 [1 + 0.749 + 0.171 + 0.053] \text{ pb}. \end{aligned} \quad (18)$$

To conclude, our best result for the fiducial Higgs cross section at  $N^3\text{LL}' + N^3\text{LO}$  for the cuts in Eq. (1) reads

$$\begin{aligned} \sigma_{\text{fid}}/\mathcal{B}_{\gamma\gamma} &= (25.41 \pm 0.59_{\text{FO}} \pm 0.21_{q_T} \pm 0.17_{\varphi} \\ &\quad \pm 0.06_{\text{match}} \pm 0.20_{\text{nons}}) \text{ pb} \\ &= (25.41 \pm 0.68_{\text{pert}}) \text{ pb}. \end{aligned} \quad (19)$$

Multiplying by  $\mathcal{B}_{\gamma\gamma} = (2.270 \pm 0.047) \times 10^{-3}$  [107–109],

$$\begin{aligned} \sigma_{\text{fid}} &= 57.69 (1 \pm 2.7\%_{\text{pert}} \pm 2.1\%_{\mathcal{B}} \\ &\quad \pm 3.2\%_{\text{PDF}+\alpha_s} \pm 2\%_{\text{EW}} \pm 2\%_{t,b,c}) \text{ fb}, \end{aligned} \quad (20)$$

where we also included approximations of additional uncertainties. The  $\text{PDF}+\alpha_s$  uncertainty is taken from the inclusive case [24, 109]. For the inclusive cross section, NLO electroweak effects give a +5% correction [110], while the net effect of finite top-mass, bottom, and charm contributions is –5% (in the pole scheme we use). We can expect roughly similar acceptance corrections for both, and therefore keep the central result unchanged but include a conservative 2% uncertainty (40% of the expected correction) for each effect. Their proper treatment requires incorporating them into the resummation framework, which we leave for future work.

*Acknowledgments.* We are grateful to Xuan Chen for providing us with the NNLOjet results and for communication about them. We would also like to thank our ATLAS colleagues for their efforts in making the preliminary results of Ref. [26] publicly available. This work was supported in part by the Office of Nuclear Physics of the U.S. Department of Energy under Contract No. DE-SC0011090 and within the framework of the TMD Topical Collaboration, the Deutsche Forschungsgemeinschaft (DFG) under Germany’s Excellence Strategy – EXC 2121 “Quantum Universe” – 390833306, and the PIER Hamburg Seed Project PHM-2019-01.

*Note added.* While finalizing this work, we became aware of complementary work computing fiducial rapidity spectra in Higgs production at  $N^3\text{LO}$  using the Projection-to-Born approach [111]. The perturbative instabilities observed there are avoided here by resumming the responsible fiducial power corrections.

- 
- [1] G. Aad *et al.* (ATLAS Collaboration), Phys. Lett. B **716**, 1 (2012), arXiv:1207.7214 [hep-ex].
  - [2] S. Chatrchyan *et al.* (CMS Collaboration), Phys. Lett. B **716**, 30 (2012), arXiv:1207.7235 [hep-ex].

- [3] G. Aad *et al.* (ATLAS Collaboration), Phys. Lett. B **726**, 88 (2013), [Erratum: Phys.Lett.B 734, 406–406 (2014)], arXiv:1307.1427 [hep-ex].
- [4] G. Aad *et al.* (ATLAS Collaboration), JHEP **09**, 112 (2014), arXiv:1407.4222 [hep-ex].
- [5] G. Aad *et al.* (ATLAS Collaboration), Phys. Lett. B **738**, 234 (2014), arXiv:1408.3226 [hep-ex].
- [6] G. Aad *et al.* (ATLAS Collaboration), JHEP **08**, 104 (2016), arXiv:1604.02997 [hep-ex].
- [7] M. Aaboud *et al.* (ATLAS Collaboration), JHEP **10**, 132 (2017), arXiv:1708.02810 [hep-ex].
- [8] M. Aaboud *et al.* (ATLAS Collaboration), Phys. Rev. D **98**, 052005 (2018), arXiv:1802.04146 [hep-ex].
- [9] G. Aad *et al.* (ATLAS Collaboration), Eur. Phys. J. C **80**, 942 (2020), arXiv:2004.03969 [hep-ex].
- [10] V. Khachatryan *et al.* (CMS Collaboration), Eur. Phys. J. C **76**, 13 (2016), arXiv:1508.07819 [hep-ex].
- [11] V. Khachatryan *et al.* (CMS Collaboration), JHEP **04**, 005 (2016), arXiv:1512.08377 [hep-ex].
- [12] V. Khachatryan *et al.* (CMS Collaboration), JHEP **03**, 032 (2017), arXiv:1606.01522 [hep-ex].
- [13] A. M. Sirunyan *et al.* (CMS Collaboration), JHEP **01**, 183 (2019), arXiv:1807.03825 [hep-ex].
- [14] A. M. Sirunyan *et al.* (CMS Collaboration), Phys. Lett. B **792**, 369 (2019), arXiv:1812.06504 [hep-ex].
- [15] A. M. Sirunyan *et al.* (CMS Collaboration), JHEP **03**, 003 (2021), arXiv:2007.01984 [hep-ex].
- [16] M. Cepeda *et al.*, CERN Yellow Rep. Monogr. **7**, 221 (2019), arXiv:1902.00134 [hep-ph].
- [17] S. Dawson, Nucl. Phys. **B359**, 283 (1991).
- [18] A. Djouadi, M. Spira, and P. M. Zerwas, Phys. Lett. B **264**, 440 (1991).
- [19] M. Spira, A. Djouadi, D. Graudenz, and P. M. Zerwas, Nucl. Phys. **B453**, 17 (1995), arXiv:hep-ph/9504378.
- [20] R. V. Harlander and W. B. Kilgore, Phys. Rev. Lett. **88**, 201801 (2002), arXiv:hep-ph/0201206.
- [21] C. Anastasiou and K. Melnikov, Nucl. Phys. B **646**, 220 (2002), arXiv:hep-ph/0207004.
- [22] V. Ravindran, J. Smith, and W. L. van Neerven, Nucl. Phys. B **665**, 325 (2003), arXiv:hep-ph/0302135.
- [23] C. Anastasiou, C. Duhr, F. Dulat, F. Herzog, and B. Mistlberger, Phys. Rev. Lett. **114**, 212001 (2015), arXiv:1503.06056 [hep-ph].
- [24] C. Anastasiou, C. Duhr, F. Dulat, E. Furlan, T. Gehrmann, F. Herzog, A. Lazopoulos, and B. Mistlberger, JHEP **05**, 058 (2016), arXiv:1602.00695 [hep-ph].
- [25] B. Mistlberger, JHEP **05**, 028 (2018), arXiv:1802.00833 [hep-ph].
- [26] ATLAS Collaboration, ATLAS-CONF-2019-029 (2019).
- [27] D. de Florian, M. Grazzini, and Z. Kunszt, Phys. Rev. Lett. **82**, 5209 (1999), arXiv:hep-ph/9902483.
- [28] V. Ravindran, J. Smith, and W. L. Van Neerven, Nucl. Phys. B **634**, 247 (2002), arXiv:hep-ph/0201114.
- [29] C. J. Glosser and C. R. Schmidt, JHEP **12**, 016 (2002), arXiv:hep-ph/0209248.
- [30] X. Chen, T. Gehrmann, E. W. N. Glover, and M. Jaquier, Phys. Lett. B **740**, 147 (2015), arXiv:1408.5325 [hep-ph].
- [31] R. Boughezal, C. Focke, W. Giele, X. Liu, and F. Petriello, Phys. Lett. B **748**, 5 (2015), arXiv:1505.03893 [hep-ph].
- [32] R. Boughezal, F. Caola, K. Melnikov, F. Petriello, and M. Schulze, Phys. Rev. Lett. **115**, 082003 (2015), arXiv:1504.07922 [hep-ph].
- [33] F. Caola, K. Melnikov, and M. Schulze, Phys. Rev. D **92**, 074032 (2015), arXiv:1508.02684 [hep-ph].
- [34] X. Chen, J. Cruz-Martinez, T. Gehrmann, E. W. N. Glover, and M. Jaquier, JHEP **10**, 066 (2016), arXiv:1607.08817 [hep-ph].
- [35] J. M. Campbell, R. K. Ellis, and S. Seth, JHEP **10**, 136 (2019), arXiv:1906.01020 [hep-ph].
- [36] X. Chen, T. Gehrmann, E. W. N. Glover, and A. Huss, JHEP **07**, 052 (2019), arXiv:1905.13738 [hep-ph].
- [37] G. Bozzi, S. Catani, D. de Florian, and M. Grazzini, Nucl. Phys. **B737**, 73 (2006), arXiv:hep-ph/0508068.
- [38] T. Becher, M. Neubert, and D. Wilhelm, JHEP **05**, 110 (2013), arXiv:1212.2621 [hep-ph].
- [39] D. Neill, I. Z. Rothstein, and V. Vaidya, JHEP **12**, 097 (2015), arXiv:1503.00005 [hep-ph].
- [40] W. Bizon, P. F. Monni, E. Re, L. Rottoli, and P. Torrielli, JHEP **02**, 108 (2018), arXiv:1705.09127 [hep-ph].
- [41] X. Chen, T. Gehrmann, E. W. N. Glover, A. Huss, Y. Li, D. Neill, M. Schulze, I. W. Stewart, and H. X. Zhu, Phys. Lett. **B788**, 425 (2019), arXiv:1805.00736 [hep-ph].
- [42] W. Bizon, X. Chen, A. Gehrmann-De Ridder, T. Gehrmann, N. Glover, A. Huss, P. F. Monni, E. Re, L. Rottoli, and P. Torrielli, JHEP **12**, 132 (2018), arXiv:1805.05916 [hep-ph].
- [43] D. Gutierrez-Reyes, S. Leal-Gomez, I. Scimemi, and A. Vladimirov, JHEP **11**, 121 (2019), arXiv:1907.03780 [hep-ph].
- [44] T. Becher and T. Neumann, JHEP **03**, 199 (2021), arXiv:2009.11437 [hep-ph].
- [45] S. Catani and M. Grazzini, Phys. Rev. Lett. **98**, 222002 (2007), arXiv:hep-ph/0703012.
- [46] M. A. Ebert, J. K. L. Michel, I. W. Stewart, and F. J. Tackmann, JHEP **04**, 102 (2021), arXiv:2006.11382 [hep-ph].
- [47] M. A. Ebert and F. J. Tackmann, JHEP **03**, 158 (2020), arXiv:1911.08486 [hep-ph].
- [48] L. Cieri, X. Chen, T. Gehrmann, E. N. Glover, and A. Huss, JHEP **02**, 096 (2019), arXiv:1807.11501 [hep-ph].
- [49] G. Billis, M. A. Ebert, J. K. L. Michel, and F. J. Tackmann, Eur. Phys. J. Plus **136**, 214 (2021), arXiv:1909.00811 [hep-ph].
- [50] M. A. Ebert, I. Moutl, I. W. Stewart, F. J. Tackmann, G. Vita, and H. X. Zhu, JHEP **04**, 123 (2019), arXiv:1812.08189 [hep-ph].
- [51] J. C. Collins and D. E. Soper, Nucl. Phys. **B193**, 381 (1981), [Erratum: Nucl. Phys.B213,545(1983)].
- [52] J. C. Collins and D. E. Soper, Nucl. Phys. **B197**, 446 (1982).
- [53] J. C. Collins, D. E. Soper, and G. F. Sterman, Nucl. Phys. **B250**, 199 (1985).
- [54] S. Catani, D. de Florian, and M. Grazzini, Nucl. Phys. **B596**, 299 (2001), arXiv:hep-ph/0008184.
- [55] J. Collins, *Foundations of perturbative QCD*, Cambridge monographs on particle physics, nuclear physics, and cosmology (Cambridge Univ. Press, New York, NY, 2011).
- [56] T. Becher and M. Neubert, Eur. Phys. J. **C71**, 1665 (2011), arXiv:1007.4005 [hep-ph].



- [57] M. G. Echevarria, A. Idilbi, and I. Scimemi, *JHEP* **07**, 002 (2012), arXiv:1111.4996 [hep-ph].
- [58] J.-Y. Chiu, A. Jain, D. Neill, and I. Z. Rothstein, *JHEP* **05**, 084 (2012), arXiv:1202.0814 [hep-ph].
- [59] J. C. Collins and T. C. Rogers, *Phys. Rev. D* **87**, 034018 (2013), arXiv:1210.2100 [hep-ph].
- [60] Y. Li, D. Neill, and H. X. Zhu, *Nucl. Phys. B* **960**, 115193 (2020), arXiv:1604.00392 [hep-ph].
- [61] C. W. Bauer, S. Fleming, and M. E. Luke, *Phys. Rev. D* **63**, 014006 (2000), arXiv:hep-ph/0005275.
- [62] C. W. Bauer, S. Fleming, D. Pirjol, and I. W. Stewart, *Phys. Rev. D* **63**, 114020 (2001), arXiv:hep-ph/0011336.
- [63] C. W. Bauer and I. W. Stewart, *Phys. Lett. B* **516**, 134 (2001), arXiv:hep-ph/0107001.
- [64] C. W. Bauer, D. Pirjol, and I. W. Stewart, *Phys. Rev. D* **65**, 054022 (2002), arXiv:hep-ph/0109045.
- [65] C. W. Bauer, S. Fleming, D. Pirjol, I. Z. Rothstein, and I. W. Stewart, *Phys. Rev. D* **66**, 014017 (2002), arXiv:hep-ph/0202088.
- [66] J.-y. Chiu, A. Jain, D. Neill, and I. Z. Rothstein, *Phys. Rev. Lett.* **108**, 151601 (2012), arXiv:1104.0881 [hep-ph].
- [67] M. A. Ebert and F. J. Tackmann, *JHEP* **02**, 110 (2017), arXiv:1611.08610 [hep-ph].
- [68] G. Billis, F. J. Tackmann, and J. Talbert, *JHEP* **03**, 182 (2020), arXiv:1907.02971 [hep-ph].
- [69] R. V. Harlander, *Phys. Lett. B* **492**, 74 (2000), arXiv:hep-ph/0007289.
- [70] P. A. Baikov, K. G. Chetyrkin, A. V. Smirnov, V. A. Smirnov, and M. Steinhauser, *Phys. Rev. Lett.* **102**, 212002 (2009), arXiv:0902.3519 [hep-ph].
- [71] R. N. Lee, A. V. Smirnov, and V. A. Smirnov, *JHEP* **04**, 020 (2010), arXiv:1001.2887 [hep-ph].
- [72] T. Gehrmann, E. W. N. Glover, T. Huber, N. Ikizlerli, and C. Studerus, *JHEP* **06**, 094 (2010), arXiv:1004.3653 [hep-ph].
- [73] M. A. Ebert, J. K. L. Michel, and F. J. Tackmann, *JHEP* **05**, 088 (2017), arXiv:1702.00794 [hep-ph].
- [74] T. Lübbert, J. Oredsson, and M. Stahlhofen, *JHEP* **03**, 168 (2016), arXiv:1602.01829 [hep-ph].
- [75] Y. Li and H. X. Zhu, *Phys. Rev. Lett.* **118**, 022004 (2017), arXiv:1604.01404 [hep-ph].
- [76] M.-X. Luo, T.-Z. Yang, H. X. Zhu, and Y. J. Zhu, *JHEP* **01**, 040 (2020), arXiv:1909.13820 [hep-ph].
- [77] M. A. Ebert, B. Mistlberger, and G. Vita, *JHEP* **09**, 146 (2020), arXiv:2006.05329 [hep-ph].
- [78] M.-x. Luo, T.-Z. Yang, H. X. Zhu, and Y. J. Zhu, *JHEP* **06**, 115 (2021), arXiv:2012.03256 [hep-ph].
- [79] S. Moch, J. A. M. Vermaseren, and A. Vogt, *Phys. Lett. B* **625**, 245 (2005), arXiv:hep-ph/0508055.
- [80] A. Idilbi, X.-d. Ji, J.-P. Ma, and F. Yuan, *Phys. Rev. D* **73**, 077501 (2006), arXiv:hep-ph/0509294.
- [81] C. F. Berger, C. Marcantonini, I. W. Stewart, F. J. Tackmann, and W. J. Waalewijn, *JHEP* **04**, 092 (2011), arXiv:1012.4480 [hep-ph].
- [82] A. A. Vladimirov, *Phys. Rev. Lett.* **118**, 062001 (2017), arXiv:1610.05791 [hep-ph].
- [83] O. V. Tarasov, A. A. Vladimirov, and A. Yu. Zharkov, *Phys. Lett. B* **93B**, 429 (1980).
- [84] S. A. Larin and J. A. M. Vermaseren, *Phys. Lett. B* **303**, 334 (1993), arXiv:hep-ph/9302208.
- [85] T. van Ritbergen, J. A. M. Vermaseren, and S. A. Larin, *Phys. Lett. B* **400**, 379 (1997), arXiv:hep-ph/9701390.
- [86] M. Czakon, *Nucl. Phys. B* **710**, 485 (2005), arXiv:hep-ph/0411261.
- [87] G. P. Korchemsky and A. V. Radyushkin, *Nucl. Phys. B* **283**, 342 (1987).
- [88] A. Vogt, S. Moch, and J. A. M. Vermaseren, *Nucl. Phys. B* **691**, 129 (2004), arXiv:hep-ph/0404111.
- [89] R. N. Lee, A. V. Smirnov, V. A. Smirnov, and M. Steinhauser, *JHEP* **02**, 172 (2019), arXiv:1901.02898 [hep-ph].
- [90] J. Henn, T. Peraro, M. Stahlhofen, and P. Wasser, *Phys. Rev. Lett.* **122**, 201602 (2019), arXiv:1901.03693 [hep-ph].
- [91] R. Brüser, A. Grozin, J. M. Henn, and M. Stahlhofen, *JHEP* **05**, 186 (2019), arXiv:1902.05076 [hep-ph].
- [92] J. M. Henn, G. P. Korchemsky, and B. Mistlberger, *JHEP* **04**, 018 (2020), arXiv:1911.10174 [hep-th].
- [93] A. von Manteuffel, E. Panzer, and R. M. Schabinger, *Phys. Rev. Lett.* **124**, 162001 (2020), arXiv:2002.04617 [hep-ph].
- [94] G. Parisi, *Phys. Lett. B* **90**, 295 (1980).
- [95] G. F. Sterman, *Nucl. Phys. B* **281**, 310 (1987).
- [96] L. Magnea and G. F. Sterman, *Phys. Rev. D* **42**, 4222 (1990).
- [97] T. O. Eynck, E. Laenen, and L. Magnea, *JHEP* **06**, 057 (2003), arXiv:hep-ph/0305179.
- [98] V. Ahrens, T. Becher, M. Neubert, and L. L. Yang, *Phys. Rev. D* **79**, 033013 (2009), arXiv:0808.3008 [hep-ph].
- [99] I. W. Stewart, F. J. Tackmann, J. R. Walsh, and S. Zuberi, *Phys. Rev. D* **89**, 054001 (2014), arXiv:1307.1808 [hep-ph].
- [100] F. Dulat, S. Lionetti, B. Mistlberger, A. Pelloni, and C. Spezzia, *JHEP* **07**, 017 (2017), arXiv:1704.08220 [hep-ph].
- [101] G. Lustermsans, J. K. L. Michel, F. J. Tackmann, and W. J. Waalewijn, *JHEP* **03**, 124 (2019), arXiv:1901.03331 [hep-ph].
- [102] M. A. Ebert, J. K. L. Michel, F. J. Tackmann, *et al.*, DESY-17-099 (2018), webpage: <http://scetlib.desy.de>.
- [103] J. Butterworth *et al.*, *J. Phys. G* **43**, 023001 (2016), arXiv:1510.03865 [hep-ph].
- [104] I. Moutl, L. Rothen, I. W. Stewart, F. J. Tackmann, and H. X. Zhu, *Phys. Rev. D* **95**, 074023 (2017), arXiv:1612.00450 [hep-ph].
- [105] I. Moutl, L. Rothen, I. W. Stewart, F. J. Tackmann, and H. X. Zhu, *Phys. Rev. D* **97**, 014013 (2018), arXiv:1710.03227 [hep-ph].
- [106] M. Bonvini, S. Marzani, C. Muselli, and L. Rottoli, *JHEP* **08**, 105 (2016), arXiv:1603.08000 [hep-ph].
- [107] A. Djouadi, J. Kalinowski, and M. Spira, *Comput. Phys. Commun.* **108**, 56 (1998), arXiv:hep-ph/9704448.
- [108] A. Bredenstein, A. Denner, S. Dittmaier, and M. M. Weber, *Phys. Rev. D* **74**, 013004 (2006), arXiv:hep-ph/0604011.
- [109] D. de Florian *et al.* (LHC Higgs Cross Section Working Group), **2/2017** (2016), 10.23731/CYRM-2017-002, arXiv:1610.07922 [hep-ph].
- [110] S. Actis, G. Passarino, C. Sturm, and S. Uccirati, *Phys. Lett. B* **670**, 12 (2008), arXiv:0809.1301 [hep-ph].
- [111] X. Chen, X. Chen, T. Gehrmann, E. W. N. Glover, A. Huss, B. Mistlberger, and A. Pelloni, (2021), arXiv:2102.07607 [hep-ph].